CRREL
REPORT 82-13

US Army Corps
of Engineers
Cold Regions Research &
Engineering Laboratory

Numerical solutions for a rigid-ice model of secondary frost heave

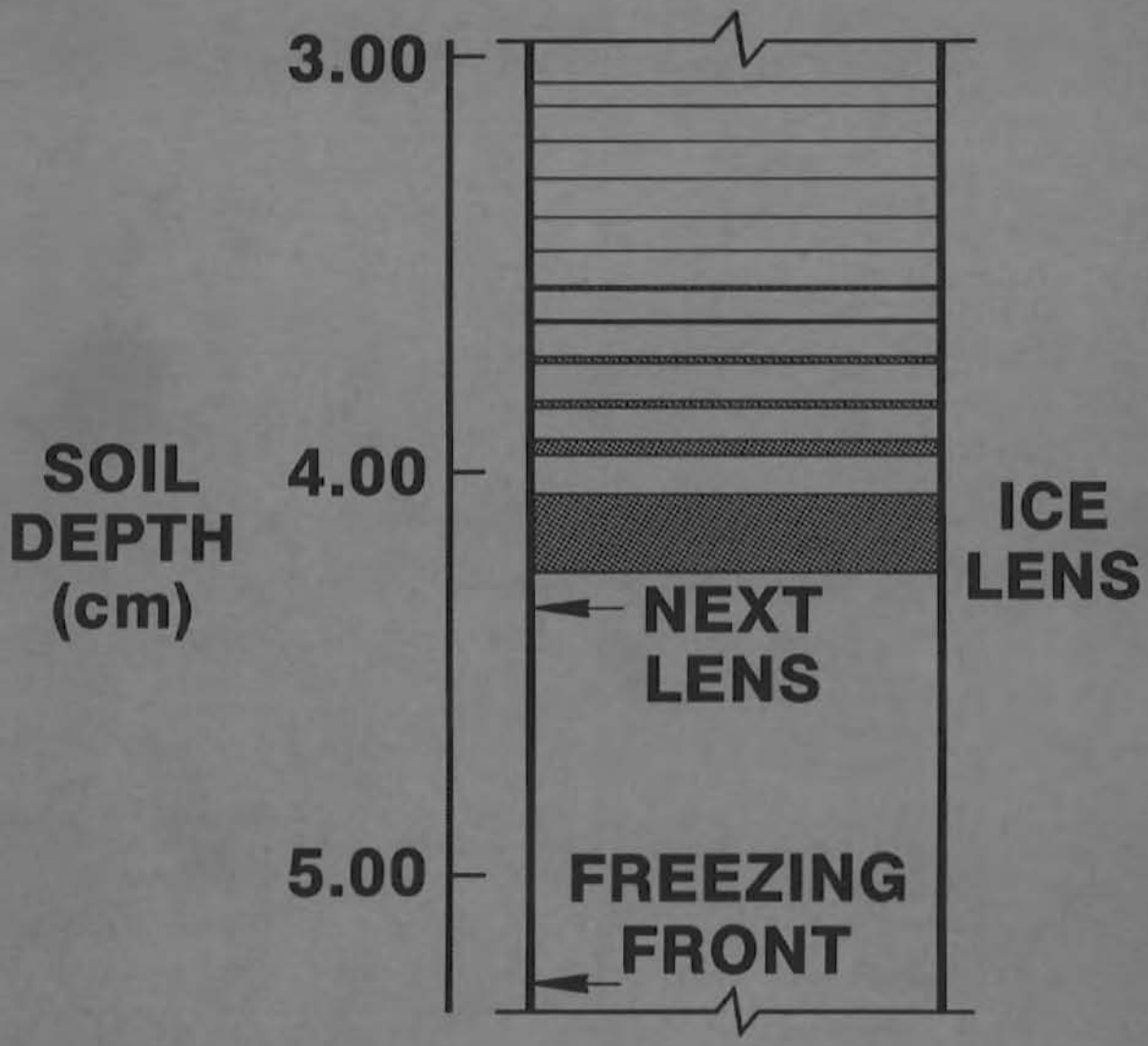

CRREL Report 82-13

April 1982

Numerical solutions for a rigid-ice model of secondary frost heave

Kevin O'Neill and Robert D. Miller

Prepared for
FEDERAL HIGHWAY ADMINISTRATION
U.S. ARMY CORPS OF ENGINEERS
FEDERAL AVIATION ADMINISTRATION

Unclassified

SECURITY CLASSIFICATION OF THIS PAGE *(When Data Entered)*

REPORT DOCUMENTATION PAGE		READ INSTRUCTIONS BEFORE COMPLETING FORM
1. REPORT NUMBER CRREL Report 82-13	2. GOVT ACCESSION NO.	3. RECIPIENT'S CATALOG NUMBER
4. TITLE *(and Subtitle)* NUMERICAL SOLUTIONS FOR A RIGID-ICE MODEL OF SECONDARY FROST HEAVE		5. TYPE OF REPORT & PERIOD COVERED 6. PERFORMING ORG. REPORT NUMBER
7. AUTHOR*(s)* Kevin O'Neill and Robert D. Miller		8. CONTRACT OR GRANT NUMBER*(s)* Intra-Governmental Order 5-3-0202; FHWA Order 8-3-0187; NSF Grant ENG-77-17004
9. PERFORMING ORGANIZATION NAME AND ADDRESS U.S. Army Cold Regions Research and Engineering Laboratory Hanover, New Hampshire 03755		10. PROGRAM ELEMENT, PROJECT, TASK AREA & WORK UNIT NUMBERS
11. CONTROLLING OFFICE NAME AND ADDRESS Federal Highway Administration, U.S. Army Corps of Engineers, and Federal Aviation Administration Washington, D.C.		12. REPORT DATE April 1982 13. NUMBER OF PAGES 17
14. MONITORING AGENCY NAME & ADDRESS*(if different from Controlling Office)*		15. SECURITY CLASS. *(of this report)* Unclassified 15a. DECLASSIFICATION/DOWNGRADING SCHEDULE

16. DISTRIBUTION STATEMENT *(of this Report)*

Approved for public release; distribution unlimited.

17. DISTRIBUTION STATEMENT *(of the abstract entered in Block 20, if different from Report)*

18. SUPPLEMENTARY NOTES

19. KEY WORDS *(Continue on reverse side if necessary and identify by block number)*

Finite element method
Freezing
Frost heave
Numerical model
Regelation
Soil

20. ABSTRACT *(Continue on reverse side if necessary and identify by block number)*

In this paper, frost heave is analyzed for the common case in which some ice penetrates the soil. In this situation, heave is due to the accumulation of soil-free ice just within the frozen zone, behind a frozen fringe of finite thickness. Heat and mass transport within and across that fringe are crucial processes in the dynamics of heave. This analysis concentrates on activity within the fringe, also connecting that activity to heat and mass flows in the more frozen and unfrozen zones. Each component in a set of governing differential equations is developed from rational physics and thermodynamics, using previous experimental work. It is assumed that the soil ice grows through interconnected interstices; hence it constitutes and can move as a rigid body. When this assumption is translated into mathematical terms, it completes the

DD FORM 1 JAN 73 1473 EDITION OF 1 NOV 65 IS OBSOLETE

Unclassified

SECURITY CLASSIFICATION OF THIS PAGE *(When Data Entered)*

20. Abstract (cont'd).

governing equations. The model resulting from these considerations is a one-dimensional finite element computer program that solves the equations for arbitrary initial and boundary conditions. The model is used to simulate the heave history of a hypothetical soil column frozen unidirectionally and subjected to a surcharge. The results are gratifying in that they predict qualitatively the characteristics of numerous laboratory observations. Some questions about the completeness of the theory remain, and strict verification of the model awaits further experimentation and better parameter identification.

PREFACE

This report was prepared by Dr. Kevin O'Neill, Research Civil Engineer, Geotechnical Research Branch, Experimental Engineering Division, U.S. Army Cold Regions Research and Engineering Laboratory, and Dr. Robert D. Miller, Professor, Agronomy Department, Cornell University. Dr. Y.C. Yen and Dr. Y. Nakano reviewed the report for its technical content.

Dr. O'Neill's participation was supported principally by joint funding from the Federal Highway Administration (FHWA), the U.S. Army Corps of Engineers, and the Federal Aviation Administration (FAA) under Intra-Governmental Order 5-3-0202. We are grateful to those (particularly Dr. Richard Berg of CRREL) who expedited this work by arranging for intermittent residence of Dr. O'Neill at Cornell and who made arrangements whereby work done on the Cornell computer could be paid for by CRREL funds, associated, in part, with FHWA Order No. 8-3-0187. The development of the model itself was supported, in part, by NSF Grant No. ENG-77-17004 to Cornell University.

This work is part of an ongoing research program. New developments, refinements, and corrections evolve continuously, and many specifics in the report may have been superseded by the time it is read. Readers are encouraged to communicate with the authors to obtain more information on latest developments.

NUMERICAL SOLUTIONS FOR A RIGID-ICE MODEL OF SECONDARY FROST HEAVE

Kevin O'Neill and Robert D. Miller

INTRODUCTION

Primary frost heave occurs when ice grows on the edge of some soil. The ice is fed by a liquid flow through the contiguous soil, but the ice does not significantly penetrate the soil. In the more common instance called secondary heave, heave proceeds when ice has penetrated the soil. A rigid-ice model of secondary frost heave in air-free, solute-free, colloid-free soils has been described both qualitatively (Miller 1977) and quantitatively (Miller 1978), but the interacting equations constituting the quantitative model have been solved only for very simple quasi-steady states (Miller and Koslow 1980). In this paper we report test case solutions of the equations, simulating the course of frost heave in a hypothetical soil column under a specified load.

The physical theory relied upon here is that in the references above. Its salient features include nonisothermal freezing, such that temperature, pressure, and ice content are all connected by a single thermodynamic relation, and each of those quantities varies continuously across the freezing zone. In addition, unfrozen moisture flows across this freezing zone, which is of finite thickness ("frozen fringe"). This flow feeds ice lens growth, which is accompanied by large, continuous changes in pressure and hydraulic conductivity across the fringe. An ice lens grows because 1) pore ice is "extruded" upward by thermally induced regelation and 2) ice forms from water moving upward through unfrozen films between the pore ice and the soil particles immediately beneath the lens. Once freezing begins, pore ice forms by accretion on pre-existing ice. Thus, all portions of ice are rigidly interconnected and move as a rigid body. The theory develops criteria in terms of thermodynamic variables for the sequential locations of lenses as freezing progresses.

GOVERNING EQUATIONS

The equations used here to simulate freezing and heaving processes come from the general laws of mass and energy conservation, together with thermodynamic and other specialized equations appropriate for saturated freezing soils. Of central importance is the expression for the pressure jump due to curvature in the liquid-water/ice interface:

$$u_i - u = \omega_{iw} \psi \qquad (1)$$

where

u = liquid pressure (N/m^2)
u_i = ice pressure (N/m^2)
ω_{iw} = ice/liquid-water interfacial tension (0.0331 N/m; Koopmans and Miller 1966).

The parameter $\psi(m^{-1})$ may be interpreted as a mean curvature of the ice/liquid interface. As some soil becomes progressively more frozen, ice penetrates smaller and smaller pores, and the average curvature of the water phase interface increases.

An equation identical to eq 1 holds for the pressure jump across the air/liquid-water interface in unfrozen, unsaturated soil, with air pressure substituted for u_i and air/water interfacial tension substituted for ω_{iw}. Pursuing this similarity, Koopmans and Miller have shown that for a given soil a "freezing characteristic curve" may be obtained, relating volumetric ice content θ_i to ψ. This curve, in turn, is related to the soil moisture characteristic curve simply by a scaling constant. In addition the parameter ψ may be expressed using a Clapeyron relation:

$$\psi = Au + BT \tag{2}$$

where T denotes temperature (°C), and the constants A and B are -2.51 m/N and -3.40×10^7 $(m°C)^{-1}$, respectively. Thus

$$\theta_i = \theta i(\psi) = \theta_i (Au + BT) . \tag{3}$$

One can use eq 3 to express the differential of θ_i as

$$d\theta_i = \left(\frac{\partial \theta_i}{\partial u}\right)_T du + \left(\frac{\partial \theta_i}{\partial T}\right)_u dT$$

$$= \left(A \frac{d\theta_i}{d\psi}\right) du + \left(B \frac{d\theta_i}{d\psi}\right) dT . \tag{4}$$

To construct a governing set of differential equations, one may begin by considering conservation of mass over a small volume element of soil, obtaining

$$\frac{\partial}{\partial t} [\rho\theta + \rho_i\theta_i] + \frac{\partial}{\partial x} [\rho v + \rho_i v_i] = 0 \tag{5}$$

where

θ = volumetric liquid content
ρ = density of liquid water ($1000 kg/m^3$)
v = liquid volume flux (m/s)
ρ_i = ice density ($917 kg/m^3$)
v_i = ice flux (m/s)
t = time(s)
x = space coordinate (m), positive downward.

The ice flux is

$$v_i = V_I \theta_i \tag{6}$$

where the ice velocity V_I (m/s) is variable in time but constant in space, in keeping with the rigid-ice assumption. We assume that liquid flux may be expressed in both freezing and unfrozen zones using a Darcy-type law:

$$v = -\frac{k}{\rho g}\left(\frac{\partial u}{\partial x} - \rho g\right) \tag{7}$$

where g is the acceleration of gravity (9.8 m/s^2) and $k(\theta_i)$ is the hydraulic conductivity (m/s). Noting that

$$\theta_i = \theta_0 - \theta \tag{8}$$

where θ_0 is the soil porosity, and incorporating eqs 6 and 7, one can rewrite eq 5 as

$$(\rho_i - \rho)\frac{\partial \theta_i}{\partial t} - \frac{\partial}{\partial x}\left[\frac{k}{g}\left(\frac{\partial u}{\partial x} - \rho g\right) - \rho_i V_l \theta_i\right] = 0\,. \tag{9}$$

For the most part, it seemed best to use eqs 3 and 4 to translate all expressions containing θ and θ_i explicitly into expressions in u and T. One can then express most physically reasonable boundary conditions relatively simply. Also, the same set of governing equations in u and T may be applied, with appropriately specified parameters, in both the unfrozen and the frozen zone. To this end, $\partial\theta_i/\partial t$ in eq 9 may be expressed using eq 4, yielding

$$\left(\Delta\rho A \frac{d\theta_i}{d\psi}\right)\frac{\partial u}{\partial t} + \left(\Delta\rho B \frac{d\theta_i}{d\psi}\right)\frac{\partial T}{\partial t} - \frac{\partial}{\partial x}\left[\frac{k(\theta_i)}{g}\left(\frac{\partial u}{\partial x} - \rho g\right) - \rho_i V_l \theta_i\right] = 0 \tag{10}$$

where $\Delta\rho$ denotes $(\rho_i - \rho)$.

Energy conservation within a small representative volume of soil provides another equation:

$$\Sigma(\rho c\theta)_n \frac{\partial T}{\partial t} - \frac{\partial}{\partial x}\left(K_h \frac{\partial T}{\partial x}\right) - \rho_i L\left(\frac{\partial \theta_i}{\partial t} + V_l \frac{\partial \theta_i}{\partial x}\right) = 0 \tag{11}$$

where

c_n = heat capacity of component n (J/kg)
K_h = soil thermal conductivity (J/m s °C)
L = latent heat of fusion of water (3.35×10^5 J/kg).

The terms $\partial\theta_i/\partial t + V_l \partial\theta_i/\partial x$ are the rate at which ice volume forms per unit volume of soil. The formation rate is not simply $\partial\theta_i/\partial t$, because ice may accumulate within a portion of the soil due to regelation heave processes, that is, due to migration as opposed to net phase change. The rate of phase change is equal to the difference between the ice accumulation rate and the in-migration rate, that is, to the sum of $\partial\theta_i/\partial t$ and $V_l \partial\theta_i/\partial x$. The particular form of these terms arises from a systematic derivation of the equation, not merely from these remarks.

Using eq 4 to reexpress $\partial\theta_i/\partial t$ in eq 11 yields

$$\left[\Sigma(\rho c\theta)_n - \rho_i L B \frac{d\theta_i}{d\psi}\right]\frac{\partial T}{\partial t} - \frac{\partial}{\partial x}\left(K_h \frac{\partial T}{\partial x}\right) - \rho_i L A \frac{d\theta_i}{d\psi}\frac{\partial u}{\partial t} - \rho_i L V_l \frac{\partial \theta_i}{\partial x} = 0. \tag{12}$$

SOLUTION PROCEDURES

If the remaining terms in eqs 10 and 12 containing V_l are reexpressed using eqs 3 and 4, then the former set becomes two equations in the unknowns u and T. In practice, the V_l terms are included in the overall u and T solution iteratively. The influence of these terms is relatively mild, so that for any current set of u and T values, θ_i expressions in the equations can be approximated

for the immediate future. This approximation is then improved, as the equations are re-solved at the same point in time for more consistent u and T values.

A finite element scheme is used for the solution in space, with simpler finite differences in time. This is frequently done in solving transport equations to treat higher derivatives in space and strongly space-dependent parameters accurately. This method has been found to be flexible and efficient for simpler freezing problems (Lynch and O'Neill 1981). In the finite element system, dependent variables are expressed as finite sums of predetermined, space-dependent interpolation ("basis") functions, each multiplied by its coefficient, which is time dependent in this case:

$$T = \sum_{j=1}^{N} T_j(t)\, W_j(x); \qquad u = \sum_{j=1}^{N} U_j(t) W_j(x). \tag{13}$$

In this study the basis functions W_j provide linear interpolation of the unknowns between mesh points, and the coefficients T_j and U_j correspond to dependent variable values at the mesh points. The problem is solved by evaluating all unknown coefficients in eq 13 through time.

Substituting eq 13 into eqs 10 and 12 and using well-established Galerkin finite element procedures (e.g. Pinder and Gray 1977) results in two coupled governing algebraic (matrix) equations, each of the general form

$$[C]\,\{\dot{V}\} + [D]\,\{V\} = \{R\} \tag{14}$$

where

$\{V\}$ = vector of unknowns, composed of both temperature and pressure coefficients
$\{\dot{V}\}$ = its time derivative
$\{R\}$ = vector containing specified quantities and the V_1 terms.

At this point the problem has been transformed into a matrix ordinary differential equation in time.

Time derivatives of the coefficients in $\{V\}$ are expressed

$$\dot{V}_j \approx \frac{V_j^{k+1} - V_j^k}{\Delta t} \tag{15}$$

where Δt is the time step size and V_j^k denotes the jth coefficient evaluated at the kth time level. The time steps may vary in size, ranging in this study from seconds as freezing begins to hours as a steady state is approached.

Using eq 15 in eq 14 results in two matrix equations of the form

$$[E]\,\{V^{k+1}\} = \{R\} - [F]\,\{V^k\}\ . \tag{16}$$

In this equation the matrices $[E]$ and $[F]$ are time dependent because they contain quantities derived from the dependent variables (e.g. $d\theta_i/d\psi$). Optimal stability was obtained with a "fully implicit" formulation, in which the matrices are evaluated at the k+1 time level, and eq 15 represents a backwards difference in time. Thus, in the course of a simulation the matrices are updated iteratively. The boundary conditions in terms of the coefficients are also incorporated in eq 16.

In general, the solution cycles may be characterized as follows: Both temperature and pressure coefficients in the V_j^k are known, either from previous analysis or from the initial conditions. On the basis of these values, $d\theta_i/d\psi$, $k(\theta_i)$, etc. are estimated, from which the matrices and R_j at the next time level are specified. The system is then solved for the V_j^{k+1} values, i.e. for the dependent variable values at the k+1 time level. These values are then used to re-estimate other dependent

quantities at t^{k+1}. The system is then solved again for a new, presumably more consistent set of V_j^{k+1} values. The process is repeated until the degree of convergence is deemed sufficient for one to proceed to the next point in time.

At any point in time, a formula for V_l is obtained in terms of the current values of u and T by taking a mass balance at the bottom of the lowest lens. Throughout the lens (including its base) ice is moving upwards with a mass flux of $\rho_i V_l$. Just below the lens, soil ice is rigidly connected to the lens ice and therefore has the same velocity V_l. However, below the lens, ice composes only a fraction of the medium cross section equal to θ_i; thus, the ice flux there is $\rho_i V_l \theta_i$. A liquid mass flux ρv also exists in the soil below the lens. Equating the mass flux entering the lens boundary from below with that leaving from above yields

$$\rho_i V_l = \rho_i V_l \theta_i + \rho v \, . \tag{17}$$

When eq 7 is substituted into eq 17, one obtains an expression for V_l:

$$V_l = -k\left(\frac{\partial u}{\partial x} - \rho g\right)/\rho_i g(1 - \theta_i) \, . \tag{18}$$

When k and θ_i are evaluated from expressions in u and T, V_l may be evaluated for use in the governing equations and in other calculations.

THE COURSE OF A SIMULATION

So far, simulations using the theory in this paper have been performed for a column 15.3 cm long. The warm end was held at 1°C and atmospheric pressure ($u = 0$); initially the entire column was considered to be uniformly at 1°C and zero gage pressure. The temperature on the freezing side soil surface was specified through all time. The boundary conditions at the freezing end varied according to the stage of the simulation, as described below.

In the first stage the freezing side surface temperature is lowered at a constant rate from 0°C. With a specified overburden pressure P, heave is temporarily restrained, and the ice velocity V_l is therefore zero. The liquid flux at the freezing end is also zero, so that one can specify a pressure boundary condtion there using eq 7:

$$(\partial u/\partial x)_{x=0} = \rho g \, . \tag{19}$$

During this stage the ice content increases, driving liquid out of the column, and the liquid and ice pressures both increase.

The second stage of the simulation begins when the ice pressure at the freezing surface (as calculated from eq 1) reaches P, so that a lens there can support the overburden. Heave and lens formation begin and V_l is nonzero. The analysis concentrates on the freezing zone below the lowest lens, where the crucial heat and mass transfer activities take place. The mesh point separations are as little as 2.5×10^{-5} m immediately below the lens, and they increase geometrically to about 3 cm at the unfrozen end. The freezing activity above the lowest lens is assumed to be slight, so that the temperature distribution there may be considered linear. This assumption was borne out by results in the mostly frozen zone before heave began. (This assumption was enlisted only as a computational convenience for the current examples and need not be employed in more sophisticated simulations based on the same theory.)

One boundary condition for the soil below the lowest lens is obtained from a heat balance across the lens boundary:

$$K_{hf}\left(\frac{T_b - T_s}{\ell}\right) = K_h\left(\frac{\partial T}{\partial x}\right)_{x=b} - L\rho v(x=b) \tag{20}$$

where

$(x = b)$ = location of the base of the lowest lens

ℓ = length of the frozen material between the soil surface and $x = b$

$T_s\ (t)$ = specified surface temperature

$T_b\ (t)$ = temperature at $x = b$

K_{hf} = thermal conductivity of the frozen material above the base lens

K_h = soil thermal conductivity below the lens.

Equation 20 expresses the fact that conductive heat fluxes on opposite sides of the lens base differ by an amount proportional to the rate of phase change as liquid flows into the lens. This equation is included with the governing equations in eq 14 as a simultaneous condition. As heave proceeds, ℓ is continually increased, both because the location of the freezing zone advances towards a steady state and because heaving transfers material to the zone above the lowest lens.

Another boundary condition at $x = b$ is provided by a force balance there. On the lens side of the boundary, the ice is subjected to the full overburden pressure P. Although ice pressure below the lens varies from P, it is nevertheless continuous across the lens boundary, so that $u_i(x=b)$ is still equal to P. Combining this information with eqs 1 and 2 provides an equation that serves as the necessary second condition at $x = b$:

$$P - u = \omega_{iw}\psi = \omega_{iw}(Au + BT)\ . \tag{21}$$

This relation is also incorporated into the governing set of equations.

An important quantity at this stage in the analysis is the neutral stress σ_n, which is taken to be a weighted combination of isotropic stresses in the two phases of pore constituent:

$$\sigma_n = \chi u + (1 - \chi)u_i\ . \tag{22}$$

The quantity $\chi(\theta_i)$ is an empirically determined stress partition parameter, specifying the relative participations of u and u_i in the resultant σ_n. As freezing progresses below $x = b$, ice content, ψ and u_i increase. At the same time, the value of u near the lens is held down in accordance with eq 21. In general, σ_n passes through a maximum somewhere beneath $x = b$ and eventually surpasses the value of P. When this happens, the pore contents alone are able to support the overburden, no supportive force is transmitted through the soil grains, and a new lens forms. In practice, σ_n was considered to surpass P when it reached a critical value σ_{cr}, approximately 1% greater than P.

With the formation of a new lens at the location of σ_{cr}, the numerical mesh is shifted downwards, so that $x = b$ coincides with the bottom of the new lowest lens. The above-freezing boundary remains fixed. The analysis is repeated, eventually another lens forms, the mesh is shifted again, and so on.

The third and last stage begins when T_s no longer decreases, in this case reaching a minimum of -0.5°C. The analysis proceeds in the same manner, as all effects slow down, asymptotically approaching a steady state. Eventually no new lenses form, and the lens growth rate V_l approaches zero. During this and other stages, the cumulative heave h at any time t is $\int_0^t V_l dt$, which may be evaluated progressively through time by simple quadrature.

CALCULATED RESULTS

As a test of reasonableness, simulations were performed over all three stages for a hypothetical soil column, as described above. The values for $\Sigma(\rho c\theta)_n$ and K_h were assumed to be 2.0×10^6 J/°C m^3 and 4.0 J/m s °C, respectively, where ice was present, and 2.8×10^6 J/°C m^3 and 3.0

J/m s °C where it was not. Gravity was neglected. (Neither the theory nor the computer program are invalidated if these assumptions are discarded.) The hydraulic conductivity $k(\theta_i)$ was assumed to be close in value to that in an unsaturated soil with the same liquid water content. It was represented as (cf. Bresler et al. 1978)

$$k(\theta_i) = k(0)\left(\frac{\theta_0 - \theta_i}{\theta_0}\right)^7 \tag{23}$$

where the porosity θ_0 is assumed to be 0.4. A convenient relation for $\theta_i(\psi)$ was adopted (Fig. 1), suggested by the data presented by Horiguchi and Miller (1980). The experimental results obtained by Snyder (1980) led us to assume that $\chi(\theta_l)$ could be represented plausibly by $(1 - \theta_i/\theta_0)^{1.5}$.

Figure 2 shows dT_L, the time elapsed between successive lens initiations, as a function of time. At t_3, T_s reaches -0.5°C and the third stage begins, during which dT_L increases markedly. The point furthest out in time represents the last lens initiation simulated, at a time when the zero degree isotherm had nearly ceased penetration. Calculated h versus time is shown in Figure 3, together with the ice ratio r_i, for times when new lenses were initiated. Here r_i equals h divided by the current length of the frozen zone ℓ. The magnitude of h increases throughout, and both quantities increase during the third stage. During that stage each quantity increases at a slower rate on an arithmetic time scale.

Similar quantities may be determined for each layer in the system. With the inception of a new lens, another layer is added to the relatively inactive zone above. That layer consists of a section of frozen soil above the new lens, together with the lens that had just grown above that soil. The final thickness of the old lens h_L divided by the total layer thickness provides a layer ice ratio r_{iL}. Figure 4 shows that r_{iL} and h_L remain relatively constant during the second stage, increasing by about one (r_{iL}) and three (h_L) orders of magnitude through stage three.

Typical profiles of u, u_i, σ_n and T at a point in time in stage three are shown in Figure 5. At this time, the maximum σ_n has just surpassed σ_{cr}, and a new lens will form where that maximum

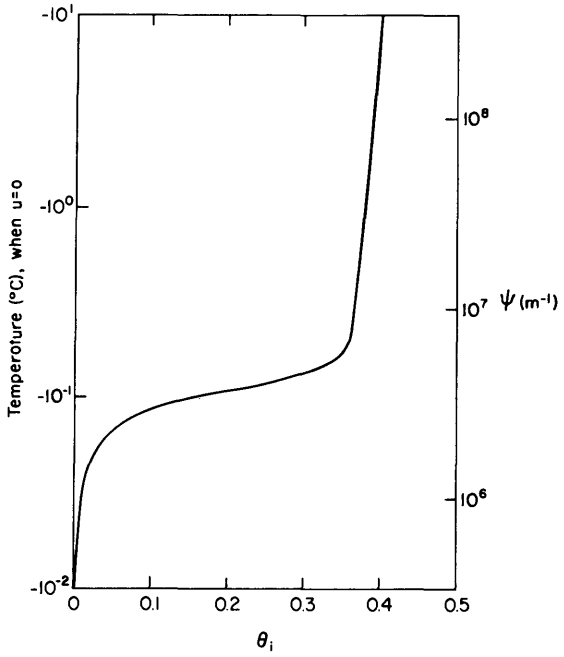

Figure 1. Ice content as a function of ψ and as a function of T *when* u = 0.

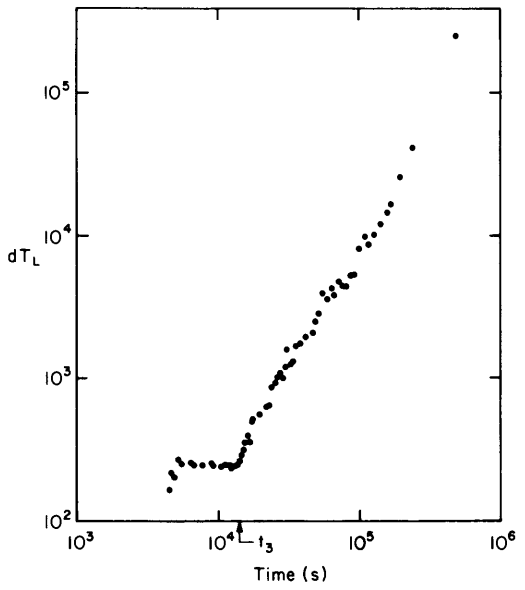

Figure 2. Time elapsed between successive lens initiations dT_L *as a function of time.*

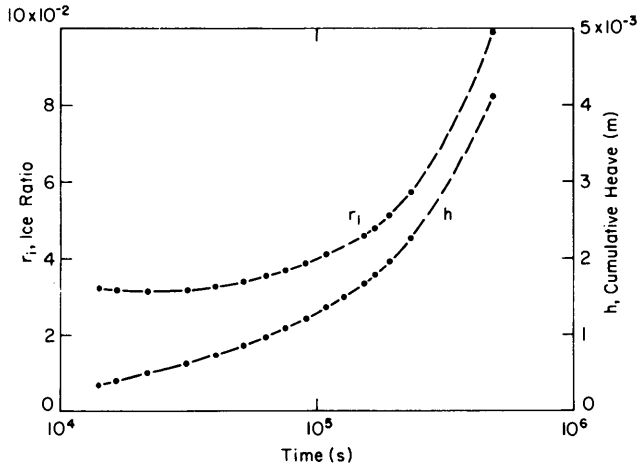

Figure 3. Calculated cumulative heave h *and ice ratio* r_i *for times when new lenses were initiated.*

exists. The liquid pressure *u* drops sharply across the freezing zone. During earlier stages freezing is more rapid as the surface temperature is lowered, and the relatively rapid formation of ice causes the liquid pressure to build up. Gradually this pressure is relieved on the freezing side as liquid flows towards the surface in conjunction with heaving and on the unfrozen side as water is expelled from the column. This leaves a maximum in between, which eventually subsides into the kind of configuration illustrated in Figure 5.

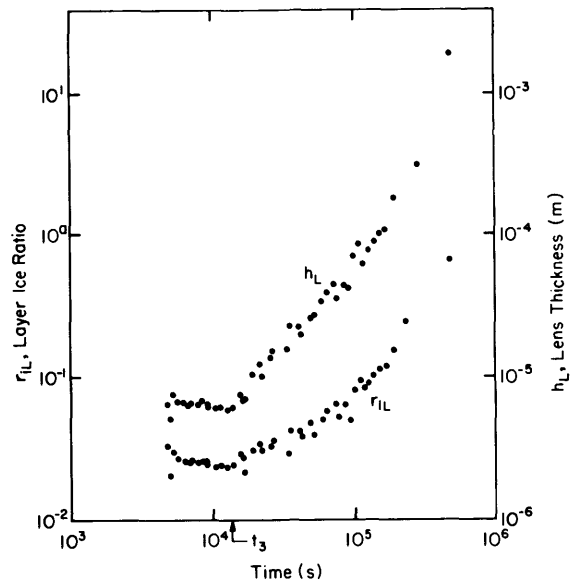

a. Lens thickness h_L and layer ice ratio r_{iL} vs time.

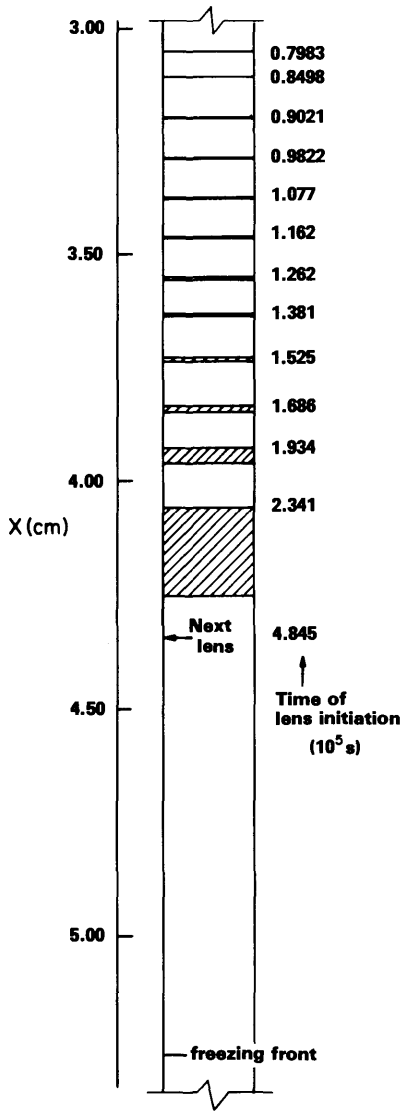

b. Lens locations (shaded) and thicknesses are shown schematically in the portion of a column. The numbers next to the lenses are their initiation times.

Figure 4. Calculated distributions of segregated ice.

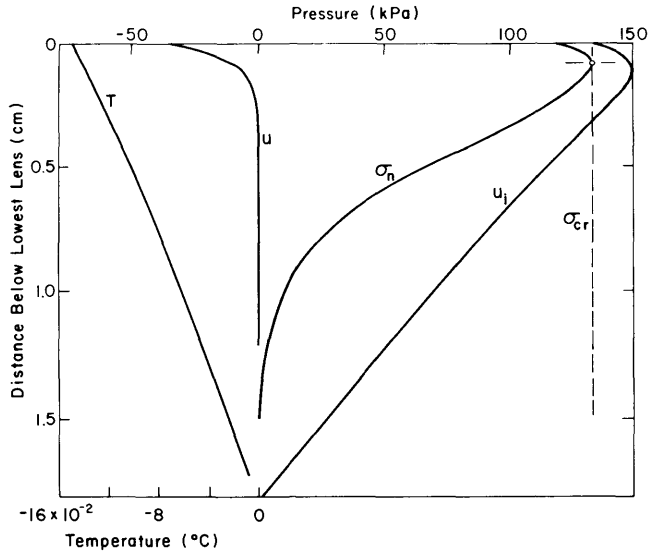

Figure 5. Profiles of u, u_i, σ_n and T at 1.38×10^5 s. The neutral stress σ_n has just surpassed the critical value σ_{cr}.

SOME PERSPECTIVE ON THE MODEL

It is gratifying to see simulations emerge from the mathematical model which are self-consistent and which are qualitatively consistent with common sense, with alternative calculations for simpler cases (Miller and Koslow 1980), and with general experience with real heaving systems. Yet questions remain. The model is based on the idea that thermally induced regelation imposes requirements for hydraulic flow in the frozen fringe and that these requirements are adequately achieved in interactions between macroscopic equations for hydraulic conductivity and thermal conductivity. The details of the microscopic recirculation of both water and heat associated with regelation are thereby left moot (cf. Miller et al. 1975). Although the approach here provides a sufficient set of equations to obtain a solution, it may leave out interactions that should be included. In other words, it is not altogether clear to us whether such microscopically based corrections are implicit in the macroscopic equations or whether virtual counterflows of water and heat must be superimposed as corrections to the macroscopic equations. If significant recirculations have not been included adequately, the real "heaving engine" may not function as effectively at high rates of heave as the model assumes. Perhaps these considerations will prove unnecessary, but it would not be altogether surprising if there were systematic discrepancies between simulations that bypass these concerns and actual heave test data.

Meanwhile, efforts to resolve the questions that lurk in our minds go forward. A recent contribution by J.R. Philip (1980) should be of great value in estimating relationships between microscopic and macroscopic thermal fields associated with regelation. Before that contribution can be exploited, however, it will be necessary to carry out a companion analysis of hydraulic impedance to regelation (a factor deliberately excluded from Philip's analysis) and to assemble these and the macroscopic function into an integrated model. Meanwhile, it seems urgent to establish a series of experiments that are controlled in a manner that can be readily simulated with the computer program as it stands or with modifications mandated by further thought and experience.

LITERATURE CITED

Bresler, E., D. Russo and R.D. Miller (1978) Rapid estimate of unsaturated hydraulic conductivity function. *Soil Science Society of America Journal,* vol. 42, p. 170–172.

Horiguchi, K. and R.D. Miller (1980) Experimental studies with frozen soil in an "ice sandwich" permeameter. *Cold Regions Science and Technology,* vol. 3, p. 177–184.

Koopmans, R.W.R. and R.D. Miller (1966) Soil freezing and soil water characteristic curves. *Soil Science Society of America Journal,* vol. 30, p. 680–685.

Lynch, D.R. and K. O'Neill (1981) Continuously deforming finite elements for solution of parabolic problems with and without phase change. *International Journal for Numerical Methods in Engineering,* vol. 17, p. 81–96.

Miller, R.D. (1977) Lens initiation in secondary heaving. *Proceedings of the International Symposium on Frost Action in Soils (Lulea),* vol. 2, p. 68.

Miller, R.D. (1978) Frost heaving in non-colloidal soils. *Proceedings of the 3rd International Conference on Permafrost (Edmonton),* National Research Council of Canada, vol. 1, p. 707–713.

Miller, R.D. and E.E. Koslow (1980) Computation of rate of heave versus load under quasi-steady state. *Cold Regions Science and Technology,* vol. 2, p. 243–252.

Miller, R.D., J.P.G. Loch and E. Bresler (1975) Transport of water and heat in a frozen permeameter. *Soil Science Society of America Journal,* vol. 39, p. 1029–1036.

Philip, J.R. (1980) Thermal fields during regelation. *Cold Regions Science and Technology,* vol. 3, p. 193–204.

Pinder, G.F. and W.G. Gray (1977) *Finite Element Simulation in Surface and Subsurface Hydrology.* New York: Academic Press.